

Secondary turbulence of parametrically excited spin waves

V. L. Grankin, V. S. L'vov, V. I. Motorin, and S. L. Musher

Institute of Automation and Electrometry, Siberian Branch of the Academy of Sciences of the USSR, Novosibirsk

(Submitted 13 February 1981)

Zh. Eksp. Teor. Fiz. **81**, 757-767 (August 1981)

The paper reports experimental and numerical-modeling studies of the mechanism underlying the onset of secondary turbulence during the parametric excitation of spin waves. It is shown that the magnetization self-oscillations in weak external magnetic pumping fields are periodic and stable against weak perturbations: a stable limit cycle exists in phase space. At high pump amplitudes the self-oscillations become irregular, and the initially close trajectories in phase space diverge exponentially. It is shown that the system of spin waves then turns out to be stable as a whole: the mean characteristics are insensitive to the wave-amplitude fluctuations.

PACS numbers: 75.30.Ds

INTRODUCTION

It is well known that a large number of interacting spin waves, i.e., parametric spin-wave turbulence, can be excited in ferromagnets with the aid of a microwave magnetic (pump) field. There arise in the process various physical effects, which have been experimentally and theoretically studied in a number of papers.^{1,2} In particular, it has been shown that the limitation of the amplitude of the parametric spin waves (PSW) is due to the interaction between the pairs of spin waves with oppositely directed wave vectors k and $-k$. Frequently, however, the steady state is not established, and the magnetization executes complex oscillations about some mean value. This phenomenon is observed in the form of amplitude and frequency modulations of the pump power passing through the resonator with the sample, or in the form of low-frequency (LF) oscillations of the z component M_z of the magnetization.

The small oscillations of the spin-wave amplitudes and phases about their steady-state values constitute, as shown in Ref. 3, a new mode of the ferromagnet's collective excitations, which is reminiscent of second-sound waves in a system of magnons. Experimentally, these collective oscillations have been detected in the resonance absorption of a weak microwave signal⁴ and a radio-frequency field.⁵ When the experimental conditions (the external magnetic field, the pump power, the reorientation of the magnetization relative to the crystallographic axes) are changed, the collective oscillation frequency may, passing through zero, become purely imaginary, so that the steady state becomes unstable.

The situation is reminiscent of the "soft-mode" type of instability that causes the phase transition in ferroelectric crystals. In our case another stable state does not occur far from the thermodynamic-equilibrium state, and the development of the soft-mode instability gives rise to magnetization self-oscillations. When the pump power is sufficiently higher than the threshold power, these oscillations have an irregular character, and we can speak of a secondary turbulence of the parametrically excited spin waves.

The question of the "nature of turbulence" and the causes of the onset of stochasticity in dynamical sys-

tems has been attracting greater and greater interest over the past ten years. The Landau model,⁶ which is based on the "self-consistent-field" idea, relates the onset of stochasticity in hydrodynamics to the successive excitation of a large number of collective degrees of freedom (e.g., of vortex motions) as the Reynolds number R increases.

There then successively appear in the Fourier spectrum at incommensurable frequencies $\omega_1, \omega_2, \dots, \omega_n$ sharp peaks that merge at $R \rightarrow \infty$ into a continuous spectrum. Another mechanism is based on the concept of "stochastic attractors" (SA), discovered by Anosov⁷ and Smale,⁸ and subsequently investigated for a number of model physical systems.⁹ A stochastic attractor is a region of attraction in the phase space of a dynamical system where there are no stable equilibrium states (poles, foci) and stable limit cycles.

Inside a SA, initially close trajectories diverge asymptotically without, however, going out of the region of attraction. As a result, the phase trajectories of the system turn out to be complicated, tangled, "stochastic," and the Fourier spectrum turns out to be continuous.

Our paper is devoted to the experimental and theoretical (with the aid of a computer) study of the mechanism underlying the development of the secondary turbulence of parametrically excited spin waves. The laboratory experiment was performed under standard conditions: the samples were good-quality single-crystal spheres of the ferromagnet yttrium iron garnet (YIG), room temperature ($T = 300$ K), pump frequency $\omega_p = 2\pi \times 9.4 \times 10^9$ sec⁻¹, $H - H_c \approx 20-50$ Oe, so that spin waves (SW) with $k \sim 10^4-10^5$ cm⁻¹ were excited, and no significant nonlinear damping occurred. The characteristics of the primary spin-wave turbulence in this parameter region are well described by S theory.² In particular, this theory predicts the experimentally observed self-oscillations stemming from the instability of the collective modes.

The numerical experiment (§1) on the S -theory equations with parameters close to the experimental parameters showed that, at low supercriticalities, the self-oscillations are strictly periodic and stable against weak perturbations, while the Fourier spectrum consists of narrow, equidistant lines corresponding to the

fundamental oscillation frequency and its multiples, i.e., the system moves in phase space along a stable limit cycle.

As the supercriticality increases, the close trajectories diverge exponentially, remaining, however, in a bounded region of phase space. This leads to the loss of the periodicity of the self-oscillations; the narrow peaks in the Fourier spectrum corresponding to the fundamental frequency and its overtones begin to broaden smoothly until they merge into a continuous spectrum at fairly high supercriticalities. It is remarkable that, despite the divergence of the close trajectories, the system of phase curves possesses "gross stability": weak fluctuations that drastically change specific solutions have little effect on their averaged characteristics, e.g., on the integrated amplitude of the waves.

In §2 we present the results of the laboratory experiment on the study of magnetization self-modulations. It is shown that the evolution of the Fourier spectrum of the self-oscillations as the amplitude of the external microwave field increases is similar to the evolution observed in the numerical modeling. It is demonstrated with the aid of a special technique that, at supercriticalities $P/P_{\text{thr}} > 2.5$ dB, the trajectories of the system of parametric spin waves diverge, and that the degree of divergence increases with increasing supercriticality.

§1. NUMERICAL MODELING

1.1. The steady state and the collective oscillations

The interaction of the spin waves plays a decisive role in the parametric excitation: it limits the level of wave excitation, and leads to the appearance of collective oscillations against its background.

The S-theory equations with allowance for the major part of this interaction have the form²

$$\begin{aligned} \frac{1}{2} \frac{\partial n_k}{\partial t} + \gamma_k n_k + \text{Im}(P_k^* \sigma_k) &= 0, \\ \frac{1}{2} \frac{\partial \sigma_k}{\partial t} + [\gamma_k + i(\tilde{\omega}_k - \omega_p/2)] \sigma_k + iP_k n_k &= 0. \end{aligned} \quad (1)$$

Here $n_k = \langle a_k a_k^* \rangle$, $\sigma_k = \langle a_k a_{-k} \rangle$ are correlation functions, the brackets denoting averaging over time or, equivalently, over the random phases of the individual waves; the a_k are the "slow" wave amplitudes; and γ_k is the decrement. The quantities $\tilde{\omega}_k$ and P_k are respectively the interaction-renormalized natural wave frequency,

$$\tilde{\omega}_k = \omega_k + 2 \int T_{kk'} n_{k'} d^3k', \quad (2)$$

and pump power,

$$P_k = \hbar V_k + \int S_{kk'} \sigma_{k'} d^3k', \quad (3)$$

where V_k is the constant characterizing the coupling between the SW and the field of the parallel pump,

$$h(t) = \hbar \exp(i\omega_p t),$$

and the $T_{kk'}$ and $S_{kk'}$ are nonlinear characteristics of the ferromagnet.

At not very large excesses over the threshold $\hbar V_{\text{thr}} = \gamma_{k, \text{max}}$ the ground steady state possesses axial sym-

metry about the direction of the magnetization M_0 (M_0 is parallel to the crystallographic axis $\langle 100 \rangle$), and the waves are disposed in the $k_z = 0$ plane, with

$$n_k^0 = \frac{N_0}{2\pi k_0} \delta(k_z) \delta(k_\perp - k_0), \quad \sigma_k^0 = n_k^0 \exp(-2i\varphi), \quad (4)$$

where $\omega_{k_0} = \omega_p/2$ and N_0 is the integrated amplitude:

$$\begin{aligned} N_0 &= \int n_k^0 d^3k = [(hV)^2 - \gamma^2]^{1/2} / |S_0|, \\ S_0 &= \frac{1}{2\pi} \int_0^{2\pi} S(\varphi) d\varphi. \end{aligned} \quad (5)$$

It is well known that there exist against the background of the ground state (4) collective oscillations with frequencies

$$\Omega_m = -i\gamma \pm [4S_m(2T_m + S_m)N_0^2 - \gamma^2]^{1/2}, \quad (6)$$

which correspond to the various modes of the azimuthal-angle motion:

$$\begin{aligned} S_m &= \frac{1}{2\pi} \int_0^{2\pi} S(\varphi) \exp(im\varphi) d\varphi, \\ T_m &= \frac{1}{2\pi} \int_0^{2\pi} T(\varphi) \exp(im\varphi) d\varphi. \end{aligned} \quad (7)$$

The $m=2$, $\text{Im } \Omega > 0$ mode turns out to be unstable in the parameter region chosen by us.² For the numerical modeling, let us choose the following simple model, which corresponds to this situation, and, as will be seen below, reproduces the main properties of the self-oscillations. Let us consider the system of SW filling two beams k_1 and k_2 in k space. In the initial state (i.e., before the pump is switched on) the wave distribution in the beams is, generally speaking, arbitrary. Let us, for definiteness, assume that $n_{1k} = \sigma_{1k} = n_0$, $n_{2k} = \sigma_{2k} = 0$. The quantity n_0 can be treated as the thermal-noise level in the SW system. The region of modulus "motion" contained on each beam

$$\Delta\omega_k = (4-6) [(hV)^2 - \gamma^2]^{1/2} \quad (8)$$

60 equally spaced points. Increases in $\Delta\omega_k$ and the number of points in this interval did not change the result.

It follows from the symmetry properties that $S_{ij} = S_{ji}^*$, $T_{ij} = T_{ji}^* = T_{ij}^*$. We shall, for simplicity, assume that the S_{ij} and T_{ij} are real; then only four of them are independent:

$$S_{12} = S_{21} = S_2, \quad S_{11} = S_{22} = S_1, \quad T_{11} = T_{22} = T_1, \quad T_{12} = T_{21} = T_2.$$

The system of equations (1)–(5) has three steady-state solutions [see (4)]:

$$\begin{aligned} 2N_1 = 2N_2 = N_0 &= [(hV)^2 - \gamma^2]^{1/2} / |S_1 + S_2|; \\ N_1^0 &= [(hV)^2 - \gamma^2]^{1/2} / |S_1|, \quad N_2^0 = 0; \\ N_1 &= 0, \quad N_2^0 &= [(hV)^2 - \gamma^2]^{1/2} / |S_1|. \end{aligned} \quad (9)$$

Let us require that the first solution be stable with respect to the $m=0$ (i.e., against a change in the sum of the amplitudes for the beams) the unstable against the induction of a difference in the amplitudes for the beams, which simulates the higher ($m \neq 0$) modes. Let us also require that the steady-state solutions lumped in one beam be stable against the excitation of oscilla-

tions in this beam. It follows from these requirements that³

$$S_0[2(T_1+T_2)+S_0] > 0, \quad (S_2-S_1)[2(T_2-T_1)+S_2-S_1] < 0, \quad (10)$$

$$S_1(2T_1+S_1) > 0, \quad S_0=S_1+S_2.$$

The specific numerical values were chosen as follows:

$$S_1=|S_0|/4, \quad S_2=3|S_0|/4, \quad T_1=-T_2=3|S_0|/8,$$

$$n_0=0.01 \left(\frac{\partial \omega}{\partial k} \Big|_{\omega_k=\omega_p/2} \right) \frac{N_0}{[(hV)^2-\gamma^2]^{1/2}}.$$

For this choice of n_0 , the regions of motion in k space where the waves grow in intensity from the noise level are not too "prolonged" in comparison with the other regions of the motion.

1.2. Procedure of the numerical experiment

The numerical simulation of the turbulence amounts to the study of the behavior of the system over time periods much longer than the characteristic periods of the motion. Therefore, the numerical solution requires the use of highly stable difference schemes that do not lead to the accumulation of computational errors over long time intervals. We used one of the variants of the Adams-Bashforth and Adams-Moulton predictor-corrector schemes.¹⁰ In the absence of self-oscillations, this method guarantees the approach to the steady-state solution (4) and a constancy of the solution to within hundredths of a percent for $t \sim (300-500)\gamma^{-1}$.

We encountered in the numerical simulation of the self-oscillations additional difficulties connected with the rapid divergence of the trajectories $n_{i,k}(t)$ ($i=1,2$) that are close in their initial values. For example, the two integral $N(t)$ curves for which the $n_{i,k}$ values at the moment of time $t=t_0$ differed by an amount of the order of n_0 , diverged completely over three self-oscillation periods when the excess $hV-\gamma=4\gamma$. The magnitude of the "confidence interval" in which the divergence of the trajectories is due to the error in the difference approximation then grew logarithmically with decreasing computational step. Thus, for the supercriticality $hV-\gamma=4\gamma$, a one-percent loss in accuracy is attained roughly by $t=32\gamma^{-1}$ (ten characteristic self-oscillation periods). This behavior remains when the predictor-corrector scheme is replaced by the Runge-Kutta method.

Generally speaking, the instability of the solutions (1) makes it impossible to study the details of the behavior of the system over time periods longer than the confidence interval. We can, however, conjecture that the set of integral curves of the system (1) possesses coarse stability, i.e., weak fluctuations that drastically change a specific trajectory $n_{i,k}(t)$ have little effect on the averaged characteristics of the solutions. The numerical experiments corroborate this hypothesis—we specifically studied the effect of random low-amplitude "impulses" on the mean amplitude and the spectrum of the power (the Fourier transform of the autocorrelation function).

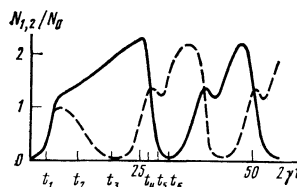


FIG. 1. Dependence of the integrated SW amplitudes in the beams 1 and 2 on the time for $hV=2\gamma$.

1.3. Discussion of the results of the modeling

Let us, to begin with, describe how the motion in k space occurs at low supercriticalities, i.e., at $hV-\gamma < 3\gamma$ [Fig. 1 shows the dependences $N_{1,2,0}(t)$ and Fig. 2 depicts the wave distribution $n_{i,k}$ at several successive moments of time]. At first, the packets $n_{i,k}$ ($i=1,2$) have the Gaussian form with the peaks at the points $\omega_k=\omega_p/2$ and grow with the increment $hV-\gamma$. As soon as $N_1 \sim N_2 \sim N_0$, instability with respect to the difference N_1-N_2 between the amplitudes begins to develop: N_2 grows more and more slowly, and then decreases ($t=t_2$). The appearance of the difference N_1-N_2 causes the packets to shift in opposite directions from the point $\omega_k=\omega_p/2$ right up to $t=t_3$, at which time $N_2 \ll N_1 \sim N_0$ and the center of the packet is at the location $\omega_k-\omega_p/2 \sim -2T_1N_1^0$. This state is, however, unstable against the production of waves in the other beam, the increment ν being maximal when $\omega_k-\omega_p/2=2T_1N_1^0$:

$$\nu_{\max} = -\gamma + \{\gamma^2 + (S_1-S_2)^2[(hV)^2-\gamma^2]/S_1^2\}^{1/2}.$$

Over the "waiting time"

$$t_4-t_3 \sim \nu_{\max}^{-1} \ln \left(\sum_k n_{2k} / N_2^0 \right)$$

the packet grows to amplitudes of the order of N_2^0 , and the difference N_1-N_2 decreases, which causes the

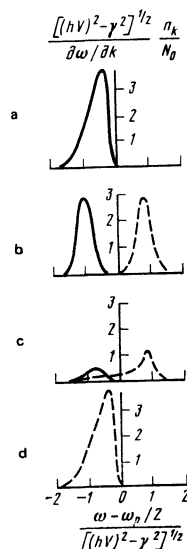


FIG. 2. Distribution of the SW in space in the beam 1 (continuous curve) and in the beam 2 (dashed curve) for $hV=2\gamma$: a) $t=t_3$, b) $t=t_4$, c) $t=t_5$, d) $t=t_6$.

packets to move back to the center $\omega_k - \omega_p/2$ and their amplitudes $N_2 > N_1$ to decrease sharply and nonuniformly. The second packet, having "survived," continues its motion in the direction of the steady state on one beam. The picture at $t = t_6$ is the same as the picture at $t = t_3$, except that the packets have exchanged places. Everything is then repeated. The characteristic swing of the motion of the packets in k space is determined by the supercriticality and the quantities T_1 and S_1 :

$$\Delta k \sim \frac{4T_1}{S_1} [(hV)^2 - \gamma^2]^{1/2} \frac{\partial \omega}{\partial k}.$$

In order to verify that the motion of the packets n_{ik} in k space is strictly periodic at low supercriticalities, i.e., that the system (1) approaches the stable limit cycle corresponding to the periodic oscillations of the total spin-wave amplitude $N = N_1 + N_2$ about N_0 , we performed the following numerical experiment.

Over a time period τ much shorter than the self-oscillation period T , the σ_{ik} values changed by an amount $\sigma_{ik}^{1/2} f_{ik}$ (whose amplitude and phase were fixed by the random-number generator with a standard deviation equal to

$$[D(f_{ik})]^{1/2} = (\tau n_0 \varepsilon \gamma)^{1/2}.$$

The step of the difference scheme was chosen such that the error in the integration over each segment of length τ did not exceed 2–3% of $[D(f_{ik})\sigma_{ik}]^{1/2}$. This method of introducing fluctuations in the case of short τ is equivalent to the action of a random force $f_{ik}(\sigma_{ik})^{1/2}$ with the correlator

$$\langle f_{ik}(t) f_{ik}(t') \rangle = \delta_{ik} \delta_{\omega} \delta(t-t') \varepsilon \gamma n_0,$$

which leads (when $hV = 0$ and $n_0 = 0$) to mean occupation numbers of the order of $n_0 \varepsilon$. Thus, the weakness of the fluctuations corresponds to $\varepsilon \ll 1$.

The system (1) was integrated for two different f_{ik} sequences (realizations) with $\varepsilon = 10^{-1}$ and $\varepsilon = 10^{-2}$. We found that the $n_{ik}(t)$ trajectories in phase space are strictly periodic and stable against weak perturbations. Thus, for $hV - \gamma = \gamma$ the $N_{1,2}(t)$ dependences obtained for different ε and f_{ik} values did not differ by more than 5% over the entire integration interval ($t \leq 40 T$). The Fourier spectrum of the autocorrelation function $|N_\Omega|^2$ consisted of a series of equally-spaced narrow peaks corresponding to the fundamental frequency of the self-oscillations and its multiples (Fig. 3a).

All this indicates that the system (1) indeed approaches a stable limit cycle at low supercriticalities. A similar method of "scrambling" the set of trajectories of the system (1) was used at higher supercriticalities. We found that, starting from $(hV - \gamma) \sim 3\gamma$, the trajectories are exponentially unstable against weak perturbations (Fig. 4), and that the mean increment of the divergence increases almost linearly with hV . The mean amplitude in this case remains finite and close to N_0 . It can be shown that there is formed in the vicinity of the limit cycle a narrow "layer" filled with exponentially unstable trajectories.

It is quite significant that the mean values of the wave amplitude and the shape of the spectrum $|N_\Omega|^2$

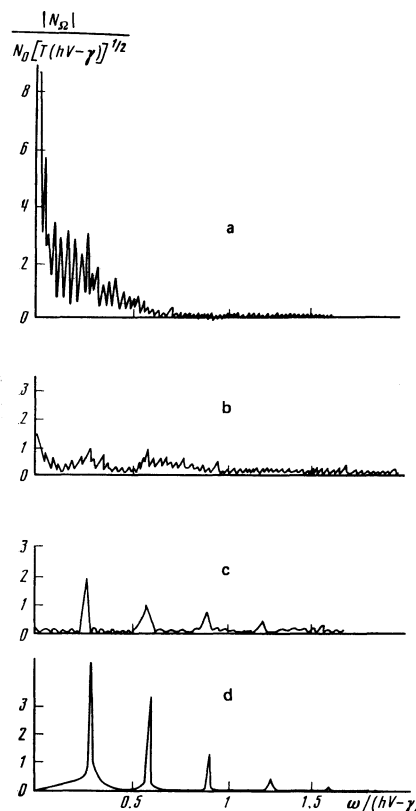


FIG. 3. Power spectrum N_ω of the integrated SW amplitude as a function of the pump power: a) $hV = 2\gamma$, b) $hV = 3.3\gamma$, c) $hV = 3.6\gamma$, and d) $hV = 9\gamma$ (numerical experiment).

turned out to be practically independent of the form of the specific realization of $f_{ik}(t)$. For example, for $hV - \gamma = 4\gamma$ and $\varepsilon = 0.1$, the quantity $\langle N \rangle$ changed by only 1% when the realization was changed, whereas the trajectories diverged fully over a time period five times shorter than the averaging time.

Let us now consider how the behavior of the trajectories in the "small" affects the behavior of the integrated spin-wave amplitude (see Fig. 3). The numerical experiment showed that it becomes more and more complicated as the supercriticality increases. Specifically, the amplitudes of the nonresonance noise Fourier harmonics begin to grow, while the sharp peaks corresponding to the frequencies $\Omega = \omega_0$, $\Omega = 2\omega_0$, etc., smoothly broaden and deform until they merge into a broad packet at $hV - \gamma = 4\gamma$ (see Fig. 3).

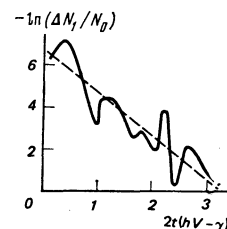


FIG. 4. Integrated-SW-amplitude difference for initially close trajectories as a function of the time (numerical experiment).

The behavior of $N(t)$ in time is interpreted as being random, stochastic.

The study of the system's motion in k space leads to the following qualitative understanding of the causes of the loss of the stability of the motion along the limit cycle. As the estimates show, the buildup increment of the oscillations $\Gamma \approx \hbar V - \gamma$, while the decrement $\delta \approx (\hbar^2 V^2 - \gamma^2)^{1/2}$. At small supercriticalities $\delta > \gamma$, and the weak perturbations have time to die down when the packet is transferred to the other beam, i.e., the oscillation-buildup process each time begins all over again. At high supercriticalities these times are comparable, complete damping of the perturbations does not occur, and the motion becomes "tangled," which leads to the loss of periodicity.

§2. THE LABORATORY EXPERIMENT

2.1. Experimental procedure

Figure 5 shows a block diagram of the experimental setup. A signal from the magnetron pump generator was fed via a number of wave-guide elements to a cavity resonator, which contained the ferrite, and was located in a constant magnetic field H . The magnetron could operate in both the continuous and pulsed regimes, and its frequency was equal to 9.4 GHz. The cavity resonator was a section of a rectangular 3-cm-band wave-guide, at one end of which was located a magnetic diaphragm coupling it to the pump circuit and at the other, near a metallic wall, the ferrite sphere under investigation. The resonator was matched with the wave guide in such a way that there was no reflection from it in the subcritical region.

There arises beyond the threshold for parametric excitation reflected radiation, which was fed to the recording circuit through a directional coupler.

The Q of the resonator was ≈ 500 , the oscillation mode was the H_{012} mode, and the microwave-magnetic-field vector was parallel to the constant field H . The recording circuit consisted of a quadratic detector, a spectrum analyzer, and a storage oscilloscope, on whose screen we could observe the frequency and temporal characteristics of the radiation reflected from the ferrite, radiation which characterized the imaginary part $\chi''(t)$ of the nonlinear susceptibility. The object of the investigation was spheres prepared from good-quality YIG single crystals of diameter 2.2 mm. The ferromagnetic-resonance line width $2\Delta H_0 \approx 0.2-0.3$ Oe

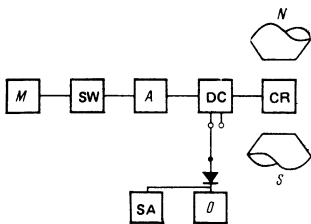


FIG. 5. Block diagram of the experimental setup: M) magnetron, SW) switch, A) attenuator, DC) directional coupler, O) oscilloscope, SA) spectrum analyzer.

and $2\Delta H_k \approx 0.15$ Oe for $k = 10^4$ cm⁻¹. The spheres were oriented by their easy axis: $H \parallel [111]$; intense self-oscillations were then observed.

2.2. Experimental results

The main measurements were performed in a field of intensity $H = H_c + 20$ Oe, when $k \sim 10^4$ cm⁻¹. The self-oscillations (SO) appeared when the excess over the parametric-excitation threshold (supercriticality) was equal to 1.8 dB. At low supercriticalities they have a periodic character with frequency $\Omega_0 = 130$ kHz. We can see on the screen of the spectrum analyzer at $\Omega = \Omega_0$ one narrow line whose width, $\Delta\Omega \leq 3 \times 10^{-2} \Omega_0$, is determined by the frequency resolution of the spectrum analyzer. As the pump power is increased, components appear at the multiple frequencies and at half-frequency. At supercriticalities $P/P_{thr} \approx 2.5$ dB the self-oscillation spectrum rapidly broadens to $\Delta\Omega/\Omega \sim 10^{-1}$.

The Fourier spectrum is an integrated characteristic characterizing the spin-wave system as a whole. Information about the behavior in the small is provided by the following experiment. Let us go over from the continuous to the pulsed parametric-excitation regime. The duration (and spacing) of the pulses is of the order of 400–500 msec, so that the SW have time to outgrow the thermal noise by several orders of magnitude. Then for the various pulses, because of fluctuations, the wave system starts each time with different initial conditions.

The $\chi''(t)$ trajectory obtained in one pulse was recorded on the screen of an oscillograph with a memory and copied on tracing paper. Then the picture was rubbed off, and the next trajectories were recorded in the same way on the same tracing paper. As a result, there is generated a strip of $\chi''(t)$ traces by which the stability of the PSW system against changes in the initial data can be judged (Fig. 6). At supercriticalities $P/P_{thr} < 2.5$ dB, the successive $\chi''(t)$ curves repeat themselves. At $P/P_{thr} \geq 2.5$ dB, when a rapid broadening of the Fourier spectrum of the self-oscillations occurs, the $\chi''(t)$ curves for the various pulses begin to diverge. Initially, the divergence of the close trajectories shows up only after long times (see Fig. 6). Then, as the supercriticality is increased, the "dispersal time" becomes comparable to the self-modulation period $\tau \sim (3-5)\Omega_0^{-1}$, and the successive $\chi''(t)$ curves form a broad band (Fig. 6c).

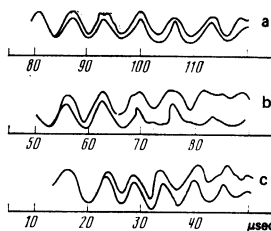


FIG. 6. Divergence of the trajectories in the natural experiment: a) $P/P_{thr} = 2.6$ dB, b) $P/P_{thr} = 2.9$ dB, c) $P/P_{thr} = 3.4$ dB.

§3. DISCUSSION OF THE RESULTS

The main measurements were performed in the parameter region where strong nonlinear damping due to the three-magnon processes does not occur. Then the nonlinear behavior of the PSW should be described by the simple S -theory equations. In particular, the theory predicts that, in YIG spheres located in $H \parallel [111]$, $S_0(2T_0 + S_0) < 0$ at room temperature, and, consequently, intense self-oscillations of the mode with the azimuthal number $m = 0$ should be excited. The threshold for the excitation of the self-oscillations should then coincide with the parametric-excitation threshold. In the experiment they differ by 1.8 dB, which is probably due to the presence of weak nonlinear damping due, for example, to the four-wave processes.

It should be said that the accurate simulation on a computer of the isotropic—in φ —self-oscillations (i.e., with $m = 0$) is difficult; for these self-oscillations cause the PSW to leave the $\theta_k = \pi/2$ plane. Consequently, the problem turns out to be two-dimensional (θ_k and $|k|$), and the required number of equations is too large. It is simpler to simulate the self-oscillations generated during the instability of the anisotropic modes (e.g., the modes with $m = 2$), when the escape from the $\theta_k = \pi/2$ plane is negligible. Since only the azimuthal harmonics with $m = \pm 2$ and $m = 0$ are nonzero in the matrix elements $T(\varphi - \varphi')$ and $S(\varphi - \varphi')$ for isotropic ferromagnets, we can take only these modes into consideration in the numerical modeling. This is equivalent to the two-beam model used by us in §1. Taking account of the fact that the self-oscillations in our laboratory experiment were due to the instability of the mode with $m = 0$, we performed check numerical experiments for the case in which the mode with $m = 0$ is unstable. They show that the qualitative properties of the self-oscillations in this case are the same as in the $m = 2$ case.

Naturally, the simple model used in the numerical modeling describes only the main properties of the self-oscillations, and cannot, of course, lay any claim to a quantitative description of the specific experimental situation in YIG. More important is the qualitative agreement between the results of the laboratory experiment and those of the numerical modeling performed with the S -theory equations, an agreement at the “conceptual” level. Specifically, in both cases the self-oscillations are periodic at low supercriticalities. The image of this motion in phase space is a stable limit cycle. Indeed, the trajectories in both the laboratory and numerical experiments turned out to be stable against small changes in the initial conditions. We have also shown that in both cases the transition to stochastic self-oscillations does not occur through the addition of new modes of motion at incommensurable frequencies, but is accompanied by the broadening of already existing spectral lines with multiple frequencies, and is due to the loss of the stability of the trajectories, which leads to their disper-

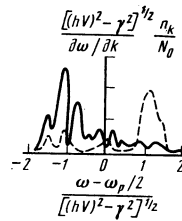


FIG. 7. Distribution in k space of the SW in the beam 1 (continuous curve) and in the beam 2 (dashed curve) for $\hbar V = 9\gamma$.

sal. This indicates that the onset of the secondary turbulence of parametric spin waves occurs in accordance with the ideas about stochastic attractors. The most important property of the model of Landau-turbulence generation, namely, the increase of the number of the effective degrees of freedom participating in the motion with increasing supercriticality, is then preserved. This is manifested in the fact that at high supercriticalities the distribution n_k (Fig. 7) is irregular, and has the form of a “picket fence” consisting of $\sim \hbar V / \gamma$ peaks.

At low supercriticalities the n_k distributions in the beams are localized packets, and the phase space contains a stable limit cycle. We can attempt to go over to a system of hydrodynamic-type equations with a small number of variables. As these variables, we can naturally choose the first moments of the distributions n_k and σ_k (the total amplitude, the center of gravity, and the width of a packet). The detailed investigation showed, however, that such a description is unsatisfactory even at very low supercriticalities, since the period, the mode, and even the very existence of the self-oscillations depend on how the chain of moments are uncoupled. We found that even a numerical uncoupling parameter does not exist, so that higher moments should be taken into consideration.

- ¹Ya. A. Monosov, *Nelineĭnyĭ ferromagnitnyĭ rezonans (Non-linear Ferromagnetic Resonance)*, Nauka, Moscow, 1971.
- ²V. E. Zakharov, V. S. L'vov, and S. S. Starobinets, *Usp. Fiz. Nauk* **114**, 609 (1974) [*Sov. Phys. Usp.* **17**, 896 (1975)].
- ³V. S. L'vov, S. L. Musher, and S. S. Starobinets, *Zh. Eksp. Teor. Fiz.* **64**, 1074 (1973) [*Sov. Phys. JETP* **37**, 546 (1973)].
- ⁴V. V. Zautkin, V. S. L'vov, and S. S. Starobinets, *Zh. Eksp. Teor. Fiz.* **63**, 182 (1972) [*Sov. Phys. JETP* **36**, 96 (1973)].
- ⁵B. I. Orel and S. S. Starobinets, *Zh. Eksp. Teor. Fiz.* **68**, 317 (1975) [*Sov. Phys. JETP* **41**, 154 (1975)].
- ⁶L. D. Landau and E. M. Lifshitz, *Mekhanika sploshnykh sred (Fluid Mechanics)*, Gostekhizdat, Moscow, 1953 (Eng. Transl., Pergamon, Oxford, 1959).
- ⁷D. V. Anosov, *Dokl. Akad. Nauk SSSR* **151**, 1250 (1963) (*sic*).
- ⁸S. Smale, *Bull. Am. Math. Soc.* **73**, 747 (1967).
- ⁹M. I. Rabinovich, *Usp. Fiz. Nauk* **125**, 123 (1978) [*Sov. Phys. Usp.* **21**, 443 (1978)].
- ¹⁰I. Babuska, *et al.*, *Numerical Processes in Differential Equations*, Wiley, 1966.

Translated by A. K. Agyei